Fast Pyrolysis of Birch Wood in a Bubbling Fluidized Bed Reactor with Recycled Non-condensable Gases

Ning Li,[a,b] Zixiang Gao,[a,b] Weiming Yi,[a,b] Zhihe Li,[a,b,*] Lihong Wang,[a,b] Peng Fu,[a,b] Yongjun Li,[a,b] and Xueyuan Bai [a,b]

A fluidized bed reactor pyrolysis process with recycled non-condensable gases was designed for a capacity of 5 kg/h based on previous basic studies of key parts. The main components of the pyrolysis process were introduced, and the performance was appraised. Initial experiments were conducted between 450 °C and 550 °C to characterize the bio-oil at different temperatures, using non-condensable gas as fluidizing medium. Simultaneously, the contents and higher heating value of non-condensable gases were determined. The results showed that the excellent efficiency of cooling and of capturing the organic compounds, contributing to a high yield of bio-oil and clean non-condensable gases. At 500 °C, the highest yield of bio-oil reached 55.6 wt%, and the yields of bio-char and gas were 23.4 wt% and 21 wt%, respectively. Non-condensable gas not only carried the organic compounds, but also participated in fast pyrolysis. However, temperature was the major factor affecting the chemical components of bio-oil. The heavy bio-oil mainly included long chain macromolecules and phenols. Higher temperature favored degradation and gas purification.

Keywords: Fluidized bed reactor; Birch wood; Fast pyrolysis; Non-condensable gas; Bio-oil

*Contact information: a: School of Agricultural Engineering and Food Science, Shandong University of Technology, Zibo, Box 255049, China; b: Shandong Research Center of Engineering and Technology for Clean Energy, Zibo, Box 255049, China; *Corresponding author: lizhihe@sdut.edu.cn*

INTRODUCTION

The high demand for fossil fuels (oil/coal/natural gas) has generated an energy crisis along with serious environmental pollution and climate change. This represents a persistent need for alternative energy resource to substitute for fossil fuels. Biomass can be acquired from plant material or derived matter through the photosynthesis reaction, including woody biomass, agricultural residues, aquatic biomass (Tripathi *et al*. 2016); animal wastes such as all types of animal manure digestate (Vassilev *et al*. 2010); and industrial wastes. As a precursor of fossil fuels, biomass can be utilized by different and efficient treatments according to its intrinsic physiochemical characterization. Fast pyrolysis is a common thermal decomposition technology that rapidly converts biomass into crude bio-oil with byproducts, bio-char, and gas at a moderate temperature and in the absence of oxygen. The relative amount of each product is in the range of liquid (50 to 70%), char (12 to 15%), and gas (13 to 25%) depending on operating parameters, properties of biomass, and type of pyrolysis reactor (Isahak *et al*. 2012). Bio-oil as a dark brown fluid liquid is composed of numerous of oxygenated organic compounds that include acids, alkanes, aromatic hydrocarbons, phenols, sugars derivatives, and small amounts of ketones, esters, ethers, and amines (Isahak *et al*. 2012). In the case of high oxygen content, corrosiveness, and high viscosity of bio-oil, additional upgrading steps

are applied with catalysts to improve the quality for heat and power supply, transportation fuels, and chemical production (such as food additives, farm insecticide, and solvents). Bio-char is also used in the tire industry as carbon soot, activated charcoal, or soil ameliorant to enhance the activity of microorganisms and absorb some harmful substances (Collard and Blin 2014; Hagner *et al*. 2015). Furthermore, it is economically viable for direct burning with the pyrolytic gas to supply heat or as the inert carrier gas for large scale plants (Lu *et al*. 2008).

With the deepening of research and improvement of the pyrolysis process, commercial plants have adopted simpler procedures and finer operation to reduce production cost and environmental impact (Kan *et al*. 2016). A fluidized bed reactor is well known in the petrochemical industry due to its characteristics of simple construction, operation, and scale-up as well as high heat/mass transfer (conduction as the main mode) (Zhang *et al*. 2010). By using an appropriate size of fluidizing bed media (sand, quartz, or catalyst) and particles (normally below 1 mm), the residence time of particles can be controlled in the range of 0.5 to 2 s by changing the gas-flow rate, which results in high yield of bio-oil (Bridgwater 2012; Isahak *et al*. 2012). The effects of pyrolysis parameters on the yield and quality of bio-oil by a micro-device under either N_2 or Ar atmosphere have been investigated (Heo *et al*. 2010). However, in pilot plants or commercial units, it is necessary to use non-condensable gas (NCG) to avoid the need for high-cost nitrogen as the initial inert carrier gas and burn the by-product char for heat supplementation; such use of NCG will improve the commercial potential of the pyrolysis process. Lu *et al*. (2008) designed a fluidized bed reactor with a capacity of 120 kg/h, which is similar to the circulating fluidized bed reactor. Their reactor is completely located within the combustion chamber, where char recycled from cyclones is burnt. However, the rate of char/air should be carefully controlled to ensure combustion efficiency. Yi *et al*. (2011) and Liu *et al*. (2009) investigated the effect of fluid bed medium and temperature on the yield and components of bio-oil under the atmosphere of hot flue gas. The fluidized gas was generated by burning anthracite with oxygen. To ensure absence of oxygen, a pivotal point was to control the ratio of air. Li *et al*. (2014) studied the effect of oxygen on products in an autothermal fluidized bed reactor. Autothermal fast pyrolysis is practical and simplifies the equipment requirements, as there is no need for external heat input. The addition of oxygen increases the production of gases such as CO and CO_2. This also changed bio-oil properties, reduced its heating value, increased its oxygen content, and increased its viscosity and phenolics concentration.

A typical NCG is composed of CO, CO_2, CH_4, and H_2, and light hydrocarbon gases, such as C_2-C_4. Theoretically, recycled NCG for fluidization can affect the decomposition of biomass in the role of a catalyst due to the reductive and oxidative gas atmosphere (Mante *et al*. 2012). Zhang *et al*. (2011) investigated biomass fast pyrolysis in a fluidized bed reactor under N_2, CO, CO_2, and CH_4 atmospheres. A CO atmosphere inhibited the bio-oil and CO and H_2 atmospheres converted much more oxygen into CO_2 and H_2O. However, the reductive atmosphere increased the HHV of bio-oil. Jung *et al*. (2008) conducted an experiment in a fluidized bed reactor under N_2 for rice straw and bamboo sawdust pyrolysis. The content of CO, CH_4, and other hydrocarbons increased with increasing temperature, and the utilization of by-product gas as a fluidizing medium enhanced the bio-oil yield. Sellin *et al*. (2016) investigated banana leaves oxidative fast pyrolysis in a fluidized bed reactor with a capacity of 12 kg/h. O_2 was the carrier gas and partially involved in combustion to maintain the energy required for biomass pyrolysis, and the inert gas ensured pyrolysis atmosphere. Furthermore, syngas was burnt to heat

the air and to reduce energy consumption. Bio-char has an intrinsic value for the activated carbon due to its high yield of char of 23.3%. Controlling the ratio of oxygen and feedstock to maximize the yield of bio-oil is an important and difficult point. Jung *et al*. (2012) studied samples of waste square timber and ordinary plywood in a bench-scale fluidized bed reactor that was equipped with gas a circulation system. They found that the amount of products is affected by NCG. However, why and how the results can be obtained still remains unclear. Heo *et al*. (2010) investigated different parameters on the effects of furniture fast pyrolysis in a small-fluidized bed reactor. The optimal temperature of fast pyrolysis was 450 °C, and the NCG increased the yield of bio-oil. The effects of temperature and particle size on the yield of bio-oil in a fluidized bed reactor with hot vapor filtration unit were investigated by Pattiya and Suttibak (2012). At 475 °C, a maximum yield of bio-oil of 69.1 wt% was obtained, and the utilization of a hot filtration unit is better for the quality of bio-oil in terms of viscosity, solids content, ash content, and stability. The addition of methanol reduces the viscosity of bio-oil and slows the ageing rates of the bio-oil.

The effect of recycled NCG in the catalytic pyrolysis of hybrid poplars using FCC catalyst was investigated in the research of Mante *et al*. (2012). The results indicated that NCG improves the content of organic liquid fraction and the quality of bio-oil. Simultaneously, the presence CO and CO_2 enhanced deoxygenation reaction, thus reducing the formation of char. Krishna *et al*. (2016) studied the pyrolysis of *Cedrus* saw-mill shavings in hydrogen and nitrogen atmosphere. Their results showed that the addition of hydrogen improved the systematic decomposition of macromolecular of biomass, which enhanced the yield of catechol. Furthermore, this promoted the efficiency of biomass fast pyrolysis. Phan *et al*. (2014) set up a fluidized bed reactor at a capacity of 60 g/h. Four types of Vietnamese biomass resources were investigated. The liquid yields were all above 50%, and the analytical results of the quality of bio-oil were satisfied, which could be directly used as combustion fuel or chemicals through upgrading. Above all, many different types of fluidized bed pyrolysis processes have been built and many parameters and different biomass were investigated. However, studies on bench-scale continuous fluidized bed pyrolysis with recycled bio-gas as the fluidized medium remain scarce.

Many problems are associated with the process such as the dynamic analysis of quench cooling (Li *et al*. 2017), the stability of the bed, and fluidizing flow rate (Li *et al*. 2015), which have been determined in previous studies. In this paper, a fast pyrolysis process based on a fluidized bed reactor coupled with a NCG circulating system was designed. The aims of this paper were (a) to build a stable and continuous process for bio-oil, for eventual scaling up; (b) to check the stability of processes according to key parameters, *e.g*., temperature, pressure, and char separation; and (c) to characterize the produced bio-oil under different operational temperatures.

EXPERIMENTAL

Biomass Preparation and Characterization

A birch wood sample grown in the Guizhou Province of China was purchased from a wood facility in Hebei Province, China. Prior to pyrolysis, it was ground and meshed to a particle size mainly in the range of 0.18 to 0.6 mm, and basic tests to

characterize the feedstock were conducted for the subsequent evaluation of biomass pyrolysis. Proximate analysis was carried out according to the ASTM E871-82 (2019), ASTM E872-82 (2019) and ASTM E1755-01 (2019) standards. Fixed carbon was calculated *via* the difference based on the content of water, volatile matter, and ash. Ultimate analysis was performed with an automatic elemental analyzer (Euro Vector, model EA 3000, Pavia, Italy) to quantify the carbon (C), hydrogen (H), and nitrogen (N) contents. Oxygen (O) content was calculated according to the formula O% =1-(C+H+N)% based on dry basis. The higher heating value (HHV) was measured *via* automatic isoperibol calorimeter (IKA, model C2000, Staufen, Germany) based on ASTM D2015-00 (2000). Every test was repeated in triplicate, and the results were averaged. Thermo-gravimetric (TG) and differential thermo-gravimetric (DTG) analyses were performed with a thermogravimetric analyzer (STA 499 F5, Netzsch, Selb, Germany). A sample of 10 mg was placed in a crucible and heated from 25 °C to 800 °C with the heating rate of 10 °C/min. Purified nitrogen (99.999%) at a flow rate of 20 mL/min was used as the carrier gas to provide an inert atmosphere and to remove the volatiles rapidly.

Pyrolysis Process Set-up and Operation

Process set-up

A pilot scale plant was designed for continuous operation with a capacity of up to 5 kg/h of biomass. Figure 1 shows the schematic diagram of the plant, which was composed of the following parts: feeding system, fluidized bed reactor, gas-solid phase separation system (two-stage cyclones), cooling and retain system, gas circulation system (roots blower, gas container and flowmeter), and automatic monitoring system.

The feeding system consisted of a hopper and two-stage screws. The hopper was designed for a throughput of 30 kg. A pipe provided a connection with the gas tank to maintain the inner pressure equilibrium and to ensure anaerobic atmosphere, when birch wood particles were continuously poured into the feeder container. An electromagnet knocker was used to avoid feedstock blockage in the hopper. The knocker was located in the wall of the hopper. The frequency of knocking the wall was altered depending on the status of feeding. The first screw was controlled to maintain feeding rate by frequency transformation. To prevent blocking, the first screw had a variable-pitch. The rotational speed of the second screw was constant at 1440 r/min, and a water-cooling tube was installed at the inlet of second screw to avoided advanced reactions before feedstock entering into the reactor. In the conjunctive location of them, a view-port was installed where the state of the discharge could be checked and where it was convenient to service the unit.

The key part of the pilot scale plant was the fluidized bed reactor, which was made of stainless steel (316S) and had an inner diameter of 120 mm. There were two main parts: an upper reaction chamber (high of 850 mm) and a lower preheater chamber (length of 700 mm) that was filled with a ceramic wafer to sufficiently preheat the carrier gas. The filler materials were randomly arranged without prejudice to the flow of gas. Quartz sand was selected as bed material with a particle size ranging between 0.6 mm and 0.8 mm. The quantity of sand and the flow rate of gas were determined in a previous study (Li *et al*. 2015). The height of the bed material was 70 mm, and the flow rate was 6 m^3/h to 8 m^3/h.

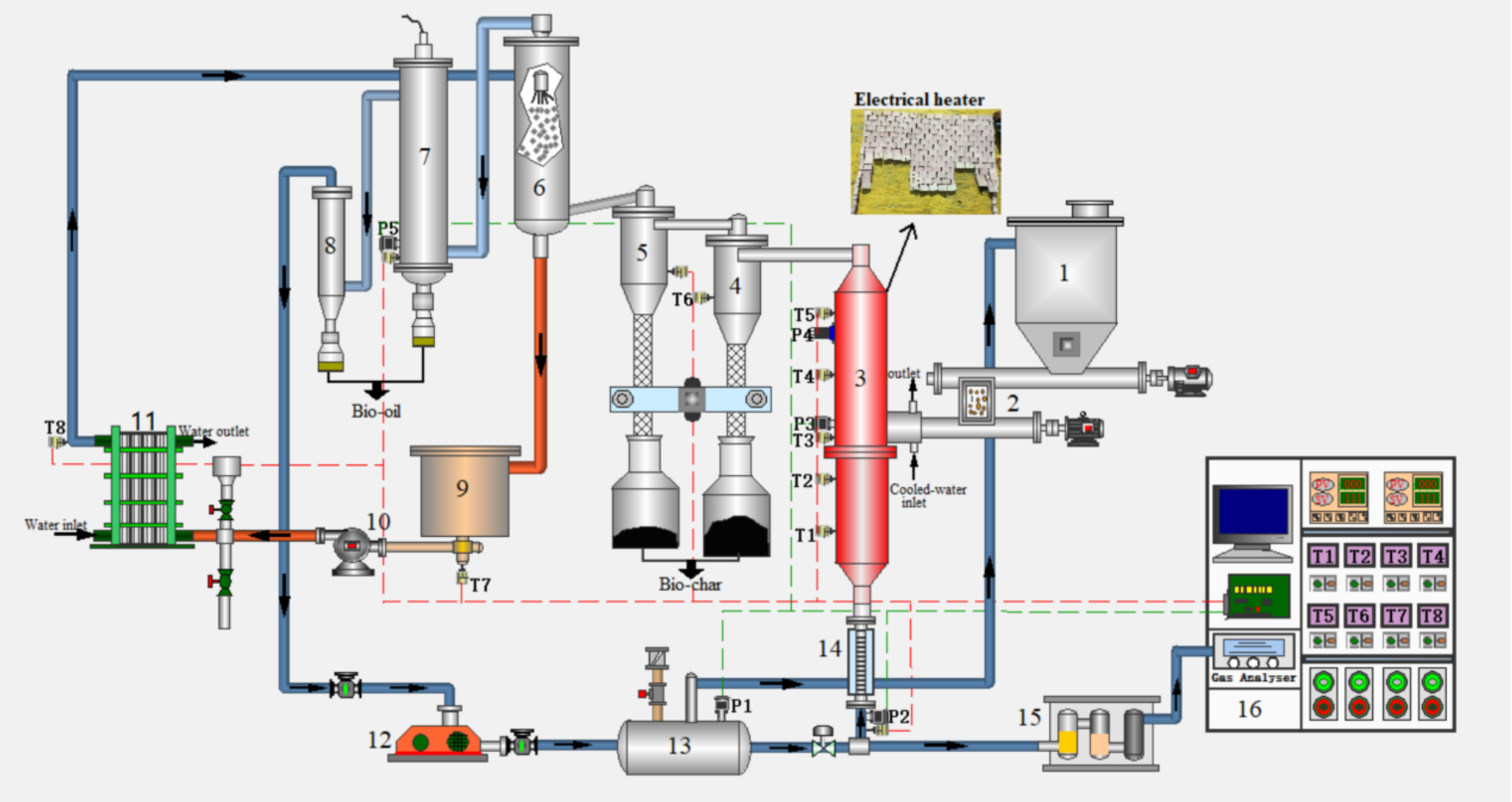

Fig. 1. The schematic diagram of 5kg/h laboratory scale plant. 1. Hopper; 2. Two-stage screw; 3. Bubbling fluidized bed reactor; 4/5. Two-stage cyclones; 6. Spray tower; 7. ESP; 8. Filter; 9. Bio-oil tank; 10. Bio-oil pump; 11. Plate heat exchanger; 12. Roots blower; 13. Gas container; 14. Rotary flowmeter; 15. Gas analyser; 16. Electric controlling and monitoring system

A cyclone is cost-effective for the separation of bio-char and vapors in industrial production. According to Fernandez-Akarregi *et al*. (2013), two-stage cyclones more effectively remove bio-char from bio-oil than one cyclone. In this paper, two-stage cyclones were connected in series, and the particle size of separated bio-char is shown in Table 2. In theory, bio-char particles bigger than 10 μm were collected. The reactor and cyclones were heated by a heating wire, which was pushed through a ceramic column. Five electric heaters were tied in the reactor and cyclones used one. Cyclones were retained at 400 °C to avoid early vapor cooling and second cracking. An electromagnetic vibrator was applied to prevent char adhering to the tube wall.

Cooling and retaining systems were used to capture organic compounds, store bio-oil, and clean NCG. The spray tower was similar to that used in a previous study (Li *et al*. 2017); however, only one spiral nozzle was used (Zhang 2012). Deionized water, ethanol, or a mixture of both was chosen as coolant contacting with hot vapor. The hot vapors were mostly collected by the first condenser at a liquid temperature of 20 °C. The bio-oil was allowed to flow to the oil pot. The non-condensable vapor of aerosols and tar was captured *via* electrostatic precipitator, which was supplied by 20 kV DC. Due to the high speed of the gas, another filter (polypropylene fiber, 0.22 μm) was used to clean the NCG. Clean NCG was sent back to the reactor *via* root blower.

All thermal sections were wrapped up in ceramic fiber material at a thickness of 150 mm, which effectively minimized heat loss. The key parts of the process were detected with a K-type thermocouple, which is shown in Fig. 1. According to the feedback information, a temperature controller equipped with proportion integration differentiation (PID) controller adjusted the appropriate temperature by changing output voltage based on the thyristor module. Considering the increasing content of gas, an electromagnetic valve mounted in the buffer tank opened automatically to vent excess gas when the pressure of system reached a fixed value. All temperature and pressure information was saved in distributed control systems (LabView and ZTIC software, Beijing, China). The concentration and HHV of NCG were recorded by a specific gas analyzer software (Wuhan, China).

Unit operation

Prior to process operation, feedstock and cooling medium were loaded, and soap bubbles were used to check the leak-tightness of conduit joints in the fast pyrolysis system. The heating system was run for fluidized bed reactor and cyclones, and the gas analyzer was started. When the temperature reached 400 °C, the root blower was operated at a low frequency and a flow rate about 4 m^3/h to improve heat exchange. Before that, the second screw should be continuously worked to prevent sand from regurgitation, which caused it to get stuck in the mechanism. After the goal temperature remained steady, the flow rate was increased to 7 to 8 m^3/h, and a small feedstock was conveyed to deplete oxygen, according to data from the gas analyzer. During the experiment, the system pressure changed with the increased gas, and the process was kept stable by altering the rotation speed of the fan. After the experiment, the first screw and the heat system were stopped; secondly, the process was run until the temperature of reactor and cyclone fell to 200 °C. After the bio-oil and bio-char were collected, cyclones were heated to partially burn adherent carbon, while the condenser system was cleaned for the next experiment.

Mass balance

The mass yield (%) of products was determined based on the ratio between the quantity of each product generated after fast pyrolysis and the quantity of the fed biomass. Before the experiment, the mass of feedstock and cooling medium were weighed as m_{fs} and m_{cm}. The quantity of bio-char was collected and weighed from a two-stage cyclone. The carbon boxes were detected to be m_{cb10}, m_{cb20}, m_{cb11}, and m_{cb21} before and after the experiment. Liquids were determined by weighing the respective mass that was obtained from spray tower (m_{Ls}), ESP (m_{Le}), and filter (m_{Lf}) after the experiments. Every experiment is given that it was at mass balance. Therefore, the pyrolysis product yields were determined with the following equations.

$$Y_{(Bio\text{-}oil)} = ((m_{Ls}+m_{Le}+m_{Lf}-m_{cm})/m_{fs}) \times 100 \quad (1)$$

$$Y_{(Bio\text{-}char)} = ((m_{cb11}+m_{cb21}-m_{cb10}-m_{cb20})/m_{fs}) \times 100 \quad (2)$$

$$Y_{(Bio\text{-}gas)} = (1-Y_{(Bio\text{-}oil)}-Y_{(Bio\text{-}char)}) \times 100 \quad (3)$$

Bio-oil and NCG analysis

The liquid fraction obtained under different temperatures was composed of light and heavy bio-oils. Chemical components were characterized *via* gas chromatography coupled with mass spectrometry (GC/MS, Agilent, Model 5973-6890N, Santa Clara, CA, USA). The content and HHV (higher heating value) of NCGes (CO, CO_2, CH_4, H_2, and light carbons) were measured *via* Gasboard-3100 gas analyzer (Wuhan Cubic Optoelectronics Co., Ltd., Wuhan, China). The HHV also can be calculated by the following formula,

$$HHV = q_1 \cdot [CO] + q_2 \cdot [CH_4] + q_3 \cdot [H_2] \quad (4)$$

Where q_1, q_2, q_3 are the HHV of CO, CH_4 and H_2, respectively (MJ/m³); [CO], [CH_4] and [H_2] are the volume concentration of gas components, respectively (vol. %).

RESULTS AND DISCUSSION

Feedstock Characterization

Table 1 lists the characteristics of the birch wood sample. The proximate analysis showed similar amounts of volatile matter and fixed carbon to woody biomass (Vassilev *et al*. 2010) of 75.8 % and 17.2 %, respectively. However, the ash content was lower than the agricultural biomass of 0.6 wt.%. This result indicated that a small amount of impurities was present, especially metal-salts, which act as catalyst and contribute to decrease of bio-oil yield and changes in the properties (Vassilev *et al*. 2010). The moisture content without drying was 6.6 %. A moisture content below 10% and a low ash content can improves heat transfer in favor of thermal conversion and reduces additional energy needs (Choudhury *et al*. 2014; Hu *et al*. 2015). Elemental analysis showed that carbon and oxygen were the fundamental components (48.52 % and 45.4 %, respectively). The HHV was 18.55 MJ/kg, which is typical for lignocellulosic biomass (Abraham *et al*. 2013). Cellulose and hemicellulose were the main components; however, the content of lignin was less compared with previous research (Jung *et al*. 2012), which could be attributed to the removal of bark in the birch wood feedstock.

Table 1. Main Characteristics of the Birch Wood Sample

Proximate Analysis (%)		Ultimate Analysis (%)		Constituents (%)	
Moisture	6.6	C	48.52	Cellulose	39.3
Volatiles	75.8	H	5.88	Hemicellulose	28.0
Fixed carbon[a]	17.2	O[a]	45.4	Lignin	23.2
Ash	0.4	N	0.2	Others[a]	8.5
HHV (MJ/kg)	18.55	S	--		

[a]:By the difference

The TG/DTG curve of birch wood in Fig. 2 indicates three thermal degradation stages between 25 °C and 800 °C. The first stage occurred prior to 200 °C, which was caused by the evaporation of water. The weight loss reached 6.24%. There are two main peaks (the temperature of peak 291 °C and 363 °C) in the second stage, which corresponded to hemicellulose devolatilization and cellulose decomposition, respectively. The maximum weight loss reached 75.4% at 520 °C. A similar peak variation and weight loss were reported by Khelfa *et al*. (2013). The third stage showed lignin decomposition and carbonization between 520 °C to 800 °C, and the loss of weight was up to 4.6%.

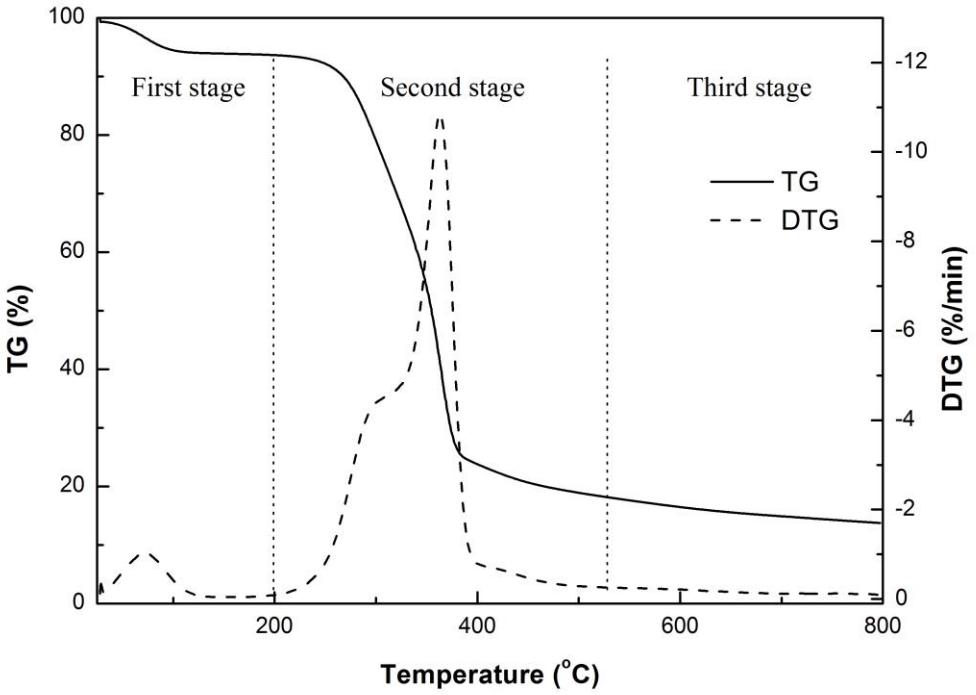

Fig. 2. TG and DTG curves of birch wood

Pyrolysis Process Stability

The temperature of key parts in the pyrolysis process is shown in Fig. 3 for a run conducted at 500 °C. The temperatures of heating parts linearly increased in the prior period, which was attributed to the lack of additional heat loss on the condition that the flowing gas was not recycled. T4 (Fig. 1) increased more sharply than others. Except for the above factor, the location was in the middle of the reactor, called the board. At 80

min, recycled flowing gas and the cooling system were started. Temperatures of the upper reactor declined due to heat taken away by gases. After 100 min, T3, T4, and T5 reached 500 °C, while T1 reached 400 °C. For the consumption of oxygen in the process, feedstock was fed into the reactor at a low feeding rate. T2 decreased to 483 °C and after 18 min, it returned to 500 °C. T1 dropped to 385 °C, which was due to the temperature change and thermal capacity of gas components and the limited heating power. Due to the excellent heat retention of the ceramic wafer, all parts of the reactor remained stable at the goal temperature. Before starting the bio-oil pump, the cooling liquid was 18 °C. Afterwards, it increased to 22 °C at 180 min, when the feeding rate was 5 kg/h. The liquid was cooled to 15.8 °C by a plate heat exchanger. This was useful for vapors quenched cooling to improve collection efficiency. Continuous operation was run for 290 min. The temperature of vapors was 506 °C, and T6 was maintained at 400 °C to reduce second cracking of volatile matter.

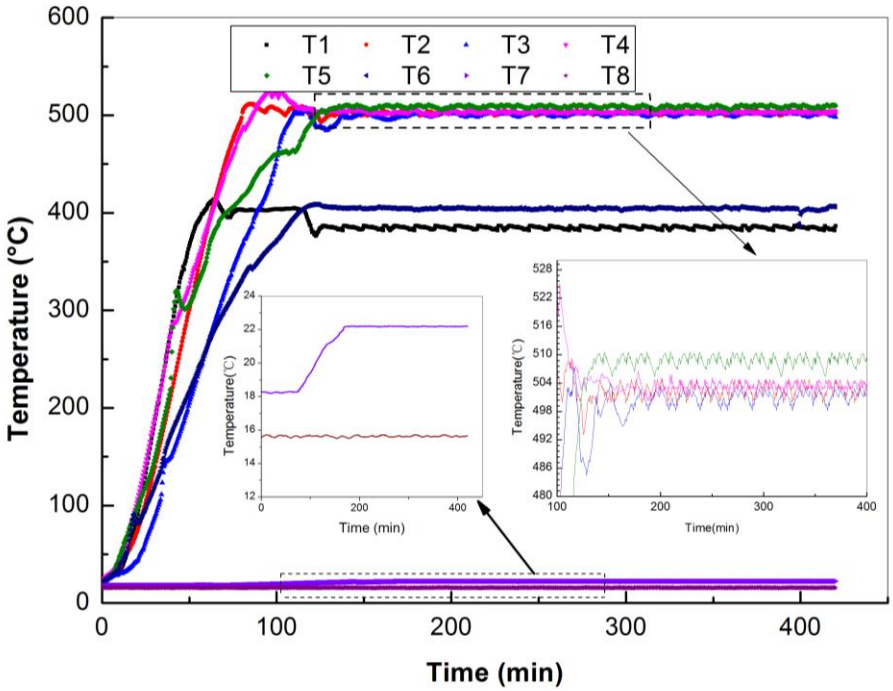

Fig. 3. The curve of temperatures in different parts throughout a continuous experiment

The pressure profiles before and during operation of the main components of the pyrolysis process are illustrated in Fig. 4. At the beginning, there was no biomass fed, and P1 and P2 (pressures shown in Fig. 1) remained stable at 3250 Pa and 3120 Pa, respectively. P3 reached 570 Pa. The pressure loss was caused by pipe friction drag and Fanning friction factor due to filler in the preheater section of the reactor. For P4, the fluidizing pressure difference was 60 Pa, which was slightly higher than the value in a previous study (Wang 2015). P5 was -1410 Pa. After feeding the biomass, all pressure values except P4 increased sharply due to the continuous increase of NCG. When the pressure of the gas container (P1) exceeded 4500 Pa, the excess gas was discharged through an electromagnetic valve opening. P1, P2, P3, and P5 reached stable values of 4500 Pa, 4500 Pa, 1740 Pa, 50 Pa, and -740 Pa, respectively. The bed pressure difference dropped slightly to about 50 Pa. Stable negative pressure in the ESP accelerated the flow speed of vapors, which was beneficial for the separation of bio-char and vapors.

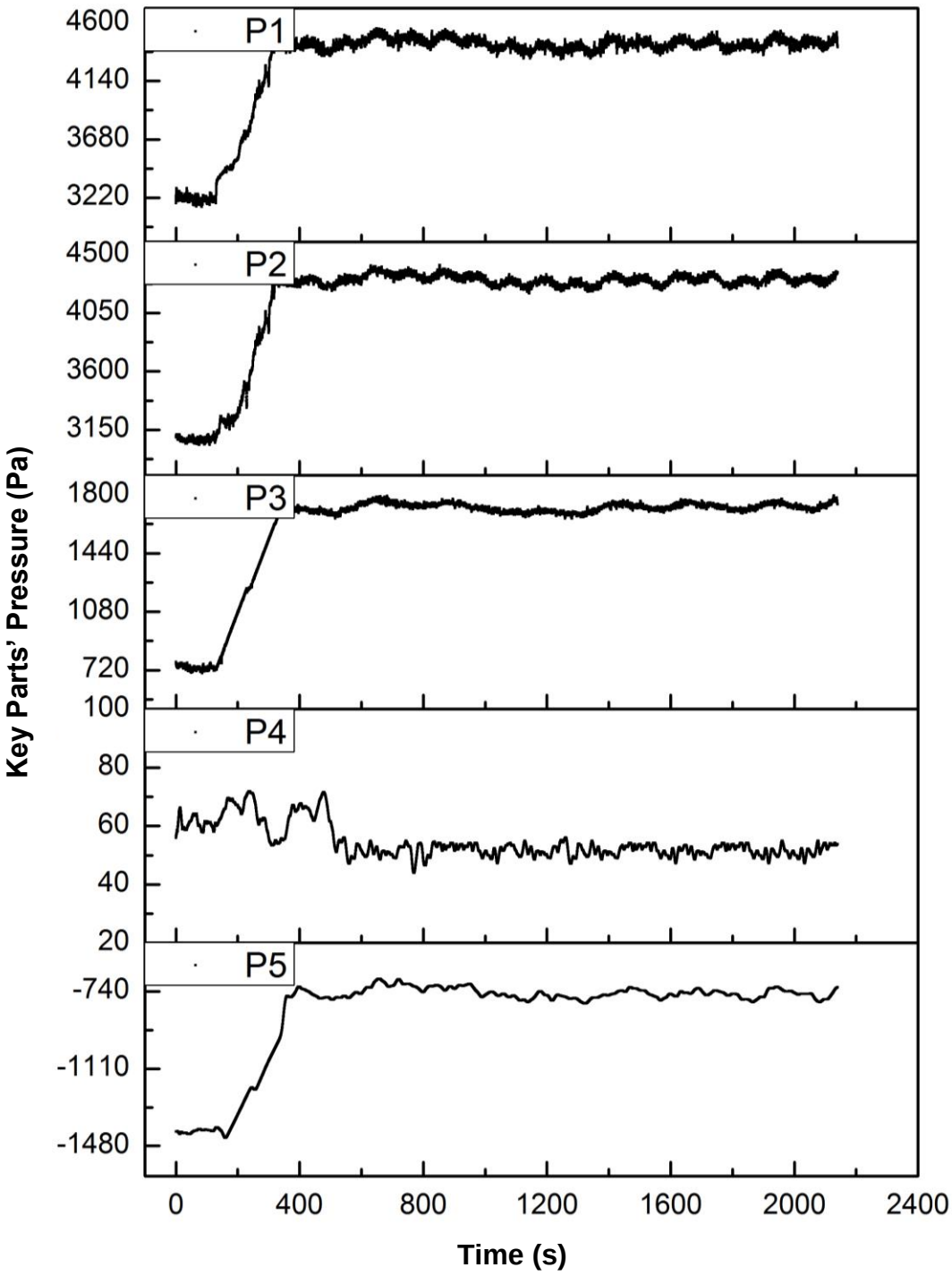

Fig. 4. The curve of pressures in different parts from beginning to stable run

Table 2. Content of Different Particle Size Distribution in Feedstock and Cyclones

Particle size	Feedstock (wt%)	Particle content in cyclones (wt%)	
		First stage	Second stage
380 <d < 600 μm	4.9	--	--
250 <d < 380 μm	60.2	16.5	--
180< d < 250μm	21.8	25.4	6.8
150 < d< 180 μm	13.1	26.8	7.3
120 < d < 150 μm	--	10.2	1.6
d < 120 μm	--	3.2	2.2
Total	100	82.1	17.9

Table 2 shows the size distribution of raw material and bio-char from two-stage cyclones. The largest amount of feedstock ranged from 0.18 to 0.38 mm. The loss of water and organic compounds of particles during pyrolysis process and the crash of bio-char and quartz sands were responsible for the distinctly narrowed size of bio-char. Hence, the size distribution of bio-char decreased to the range of 0.15 mm to 0.25 mm. Moreover, the first-stage cyclone played a decisive role in the separation of bio-char, which was up to 82.1 wt% of total bio-char collection. The second-stage cyclone as an additional supplement efficiently removed char from vapors. However, fractional ultrafine particles could not be removed, and they inevitably entered the bio-oil through quenched cooling.

Preliminary Pyrolysis Trial Results

Figure 5 presents the samples of light and heavy bio-oils. Light bio-oil had a red brown color and was thin; it contained small molecule organic matter mixed with cooling media. The heavy bio-oil was a black brown viscous liquid with fine char particles. Bio-oil emits an acrid and smoky odor.

Fig. 5. Light (a) and heavy (b) bio-oil from birch wood pyrolysis

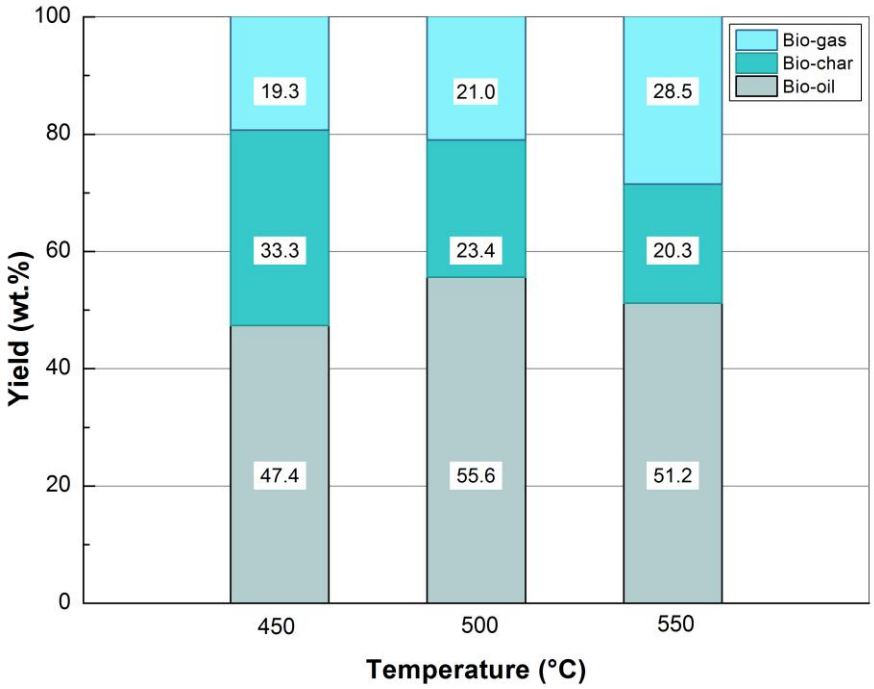

Fig. 6. Pyrolysis products yield at different temperature

The results of relative yields of pyrolysis products under different reaction temperatures were calculated, and results are shown in Fig. 6. At low temperature, the fraction of bio-oil, bio-char, and NCG obtained were 47.4 wt%, 33.3 wt%, and 19.3 wt%, respectively. By increasing the pyrolysis temperature, bio-oil yield gradually increased first and then decreased, while the yield of bio-char decreased; the gas fraction also increased. The maximum yield of bio-oil was 55.6 wt% at 500 °C. The change of bio-oil and bio-char was more obvious from 450 to 500 °C. The yield of NCG changed in the opposite way. Its content sharply increased from 21 wt% to 28.5 wt%. One factor that contributed to this phenomenon was the formation of the second cracking of vapors at a higher temperature. However, bio-char as the catalyst interacted with vapors, which contributed to an increase of NCG yield, while decreasing that of bio-char.

Although the existing CO atmosphere promoted the reaction of oxygen in the vapor, transferring it into NCG, other gases (H_2, CH_4, and CO) and temperatures may have a decisive effect on the bio-oil yield. Similar effects of the final pyrolysis temperature on the yields of products were achieved in other studies (Pattiya 2011; Abraham *et al*. 2013; Wang 2015). In these studies, various types of organic wastes were used in different reactors. Demiral and Kul (2014) investigated the effect of pyrolysis temperature on the yield of products from 400 to 550 °C. Although the yield of bio-oil was low, the trend showed an increase until 500 °C, followed by a decrease. The maximum yield of bio-oil, bio-char, and bio-gas were 21.4 wt%, 35.2 wt%, and 38 wt%, respectively. Raja *et al*. (2010) used jatropha oil cake to show that the oil yield increased from 42.2 wt% to 64.2 wt% as the temperature increased from 350 to 500 °C, and then it decreased to 57.7% at 550 °C. Claudio *et al*. (2013) studied the pyrolysis of *Astrocaryum*

aculeatum seeds in a bubbling fluidized bed reactor; the maximum bio-oil yield of 56.5 wt% was obtained at 500 °C. Phan *et al*. (2014) described the pyrolysis of rice straw in a fluidized bed reactor. The maximum bio-oil was 52.7 wt% at 500 °C. The fraction of bio-char decreased slightly, while that of bio-gas slightly increased from 470 to 500 °C. However, the yield of biogas increased sharply after 500 °C. Similar effects of temperature on the pyrolysis of cassava rhizome in a fluidized bed reactor incorporated with a moving-bed granular filter were found (Paenpong and Pattiya 2016). Compared to the yield of bio-char and bio-gas, the yield of bio-oil changed slightly.

As the experiment proceeded, the concentration of components of biogas tended to reach a stable value. The gas composition detected through a gas analyzer included CO_2, CO, H_2, and some light hydrocarbons (CH_4 and C_2-C_4) under different pyrolytic temperatures, as plotted in Fig. 7. The formation of CO_2 was caused by the cracking and reforming of functional groups of carboxyl C=O and COOH (Collard and Blin 2014). The gas release was divided into two stages, attributed to hemicellulose at less than 500 °C and lignin above 550 °C, while cellulose had a small contribution at the low temperature. The CO release was generated by the cracking of carbonyl (C=O). Below 550 °C, the partial fraction of CO was released from hemicellulose and cellulose. At a higher temperature, a larger amount of CO emerged from hemicellulose and lignin. Due to decomposition of methoxyl (-O-CH_3) and aromatic rings, CH_4 was released at low temperature (< 600 °C) from three constituents, especially for lignin (Yan *et al*. 2005). H_2 originated from the cracking and deformation of C=C and C-H groups at a higher temperature (Azargohar *et al*. 2013; Zhao *et al*. 2016).

Figure 7 shows the concentration of the components of NCG. The dominant components were CO and CO_2, which concentration addition ranged around 86 vol% at low temperature. With the increase of pyrolysis temperature, CO_2 concentration declined to 39.8 vol% at 550 °C, whereas that of CO increased to 35.2 vol%. However, the CO_2 content was always higher than that of CO. This result may be caused by the reaction of CO with oxygen in the vapors to produce more CO_2. At higher temperature, more energy poured into the reactor, which accelerated the rupture of C-C and C=C and the secondary cracking of vapors. The H_2, CH_4, and light hydrocarbon contents increased. Compared with the other gases (CH_4 and C_nH_m), H_2 increased noticeably (3.8 to 8.6 vol%). The highest content of CH_4 was 13.8% at 550 °C. C_nH_m did not change significantly in the range of 1.8 and 2.6 vol%. The yield of NCG (except CO_2) determined the calorific value of the gas. This value was critically affected by the content of CO and CH_4. As temperature increasing, HHV of NCG increased from 6.8 MJ/m³ to 11.2 MJ/m³.

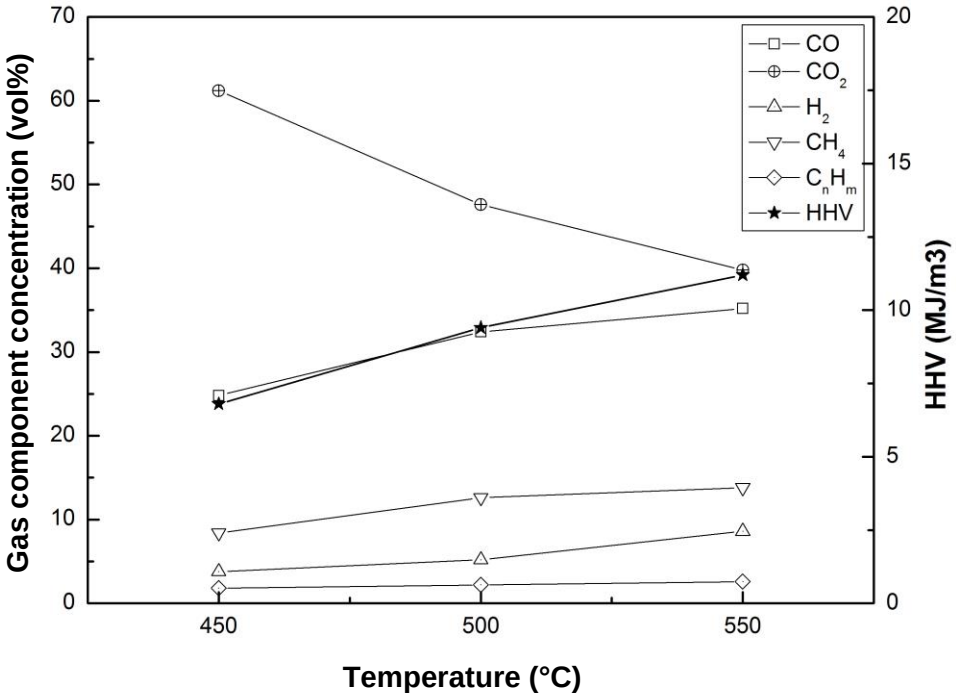

Fig. 7. The contents and HHV of recycled non-condensable gas

Table 3 shows the relative content of light bio-oil under different temperatures. The components were classified in ten groups including acids, esters, aldehydes, alcohols, ketones, phenols, ethers, sugars, and nitrogen compounds.

Acid was one of the main components of bio-oil. With increasing temperatures, its content decreased from 9.21% to 13.37%. The trend was similar to a previous study (Heo *et al*. 2010). However, due to the high content of CO_2 at low temperature, it contributed to acid through two possible ways: CO_2 and CO will react with reactive volatiles and can also react with solid residues to produce acids. Furthermore, light oxygenates originate from the decomposition of anhydro saccharides.

Phenols are the most important part of bio-oil and result from the pyrolyzed of lignin. With temperature increasing, phenols increased to the highest content of 29.2% at 550 °C. CO was found to promote demethoxylation of lignin by the means of reacting with the aromatic C-O bond (Mante *et al*. 2012). Hence, due to the gas medium of CO and CO_2, especially for the increased content of CO, less oxygen-containing groups of compounds were produced, and more monofunctional phenols were generated. At 550 °C, relatively higher H_2 content produced more methoxy-containing compounds which enhanced the formation of polymerization precursor. But the relative lower content compare with CO and CO_2 caused a non-significant variation of methoxy-phenols.

Table 3. Chemical Compounds in Light and Heavy Bio-oil of Birch Wood under Different Temperatures

Compound	Formula	Area (%) in light bio-oil		
		450 °C	500 °C	550 °C
Acids				
Acetic acid	$C_2H_4O_2$	6.56	7.25	8.26
Propanoic acid	$C_3H_6O_2$	1.26	3.62	3.88
ç-Hydroxy, butyric acid	$C_4H_8O_3$	0.52	0.24	--
Total		8.34	11.11	12.14
Esters				
Methyl formate	$C_2H_4O_2$	1.56	1.73	1.53
Acetic acid, methyl ester	$C_3H_6O_2$	1.8	2.03	1.96
Formic acid, ethyl ester	$C_3H_6O_2$	2.75	2.82	3.3
5-Oxotetrahydrofuran-2-carboxylic acid, ethyl ester	$C_7H_{10}O_4$	0.22	0.28	--
Total		6.33	6.76	6.79
Phenols				
Phenol	C_6H_6O	3.82	4.25	4.94
1,2-Benzenediol	$C_6H_6O_2$	2.96	3.6	4.35
Hydroquinone	$C_6H_6O_2$	--	0.43	0.82
Phenol, 4-methyl-	C_7H_8O	2.26	3.84	4.82
Phenol, 2-methyl-	C_7H_8O	2.28	2.96	3.68
Phenol, 2-methoxy-	$C_7H_8O_2$	1.1	1.45	1.64
Phenol, 2-methoxy-4-methyl-	$C_8H_{10}O_2$	--	0.5	0.34
Phenol, 2,6-dimethoxy-	$C_8H_{10}O_3$	1.26	2.12	2.66
Vanillin	$C_8H_8O_3$	2.62	1.62	0.81
2-Methoxy-4-vinylphenol	$C_9H_{10}O_2$	2.32	1.71	0.86
1,2,4-Trimethoxybenzene	$C_9H_{12}O_3$	1.96	1.54	1.22
Phenol, 2-methoxy-5-(1-propenyl)-, €-	$C_{10}H_{12}O_2$	0.55	0.81	--
Phenol, 2-methoxy-4-propyl-	$C_{10}H_{14}O_2$	2.22	1.56	1.44
Phenol, 4-(3-hydroxy-1-propenyl)-2-methoxy-	$C_{10}H_{12}O_3$	--	0.25	0.19
Phenol, 2,6-dimethoxy-4-(2-propenyl)-	$C_{11}H_{14}O_3$	0.66	1.31	1.45
Total		24.01	27.95	29.22
Aldehydes				
2-Furancarboxaldehyde, 5-(hydroxymethyl)-	$C_6H_6O_3$	1.22	1.44	1.38
Benzaldehyde, 3-hydroxy-4-methoxy-	$C_8H_8O_3$	0.36	0.65	0.76
Hexanal, 2-ethyl-	$C_8H_{16}O$	0.22	0.19	0.45
4-Hydroxy-2-methoxycinnamaldehyde	$C_{10}H_{10}O_3$	1.54	1.26	1.05
Total		3.34	3.54	3.64
Ketones				
2-Cyclopentene-1,4-dione	$C_5H_4O_2$		0.19	
1,2-Cyclopentanedione	$C_5H_6O_2$	2.22	2.62	4.52
3-Pentanone	$C_5H_{10}O$	2.85	3.32	4.85
2,2-Dimethyl-3-heptanone	$C_9H_{18}O$	1.32	1.61	2.45
Ethanone, 1-(2-hydroxy-5-methylphenyl)-	$C_9H_{10}O_2$	1.45	0.95	1.22
Xanthosine	$C_{10}H_{12}N_4O_6$	1.33	1.00	0.33
Ethanone, 1-(4-hydroxy-3-methoxyphenyl)-	$C_9H_{10}O_3$	1.25	1.61	1.02
Total		10.42	11.11	14.39
Furans				

3-Furaldehyde	$C_5H_4O_2$	2.06	3.69	4.55
2-Furanmethanol	$C_5H_6O_2$	1.21	2.32	3.12
2(5H)-Furanone	$C_4H_4O_2$	0.85	1.92	2.45
5-Hydroxy-methyl-dihydro-furan-2-one	$C_5H_8O_3$	1.05	1.21	0.66
4-Methyl-5H-furan-2-one	$C_5H_6O_2$	0.15	0.26	0.45
2-Furancarboxaldehyde, 5-methyl-	$C_6H_6O_2$	0.3	0.5	1.2
2(5H)-Furanone, 5-methyl-	$C_5H_6O_2$	0.2	0.27	0.65
2(5H)-Furanone, 3-methyl-	$C_5H_6O_2$	0.1	0.23	0.65
Furfural	$C_5H_4O_2$	1.98	3.34	3.55
Total		8.62	13.74	17.65
Nitrogen compounds				
N-Nitrosodimethylamine	$C_2H_6N_2O$	0.65	0.72	0.75
2-Imidazolidinethione	$C_3H_6N_2S$	0.66	0.69	0.79
Ethanol, 2-nitro-, propionate (ester)	$C_5H_9NO_4$	1.28	1.45	1.48
N-Butyl-tert-butylamine	$C_8H_{19}N$	0.52	0.73	0.65
Oxazolidine, 2,2-diethyl-3-methyl-	$C_8H_{17}NO$	1.44	1.52	1.68
Total		4.55	5.11	5.35
Saccharides				
1,6-Anhydro-á-D-glucopyranose (levoglucosan)	$C_6H_{10}O_5$	13.3	7.4	4.8
1,4:3,6-Dianhydro-à-d-glucopyranose	$C_6H_8O_4$	0.42	0.45	--
Sucrose	$C_{12}H_{22}O_{11}$	2.12	1.17	0.48
Total		15.84	9.02	5.28
Alcohols				
Cyclobutane methanol	$C_5H_{10}O$	0.68	0.80	1.2
Ethanol, 2,2-diethoxy-	$C_6H_{14}O3$	0.25	0.37	0.56
Cyclohexanol, 4-methyl-, cis-	$C_7H_{14}O$	0.66	0.92	0.98
Benzyl alcohol, à-(1-(dimethylamino)ethyl)-	$C_{11}H_{17}NO$	0.18	0.25	0.32
3-Benzo furan methanol, 2,3-dihydro-2-(4-hydroxy-3-methoxyphenyl)-5-(3-hydroxy-1-propenyl)-7-methoxy-	$C_{20}H_{22}O_6$	0.33	0.28	--
Total		2.1	2.62	3.06
Aromatics				
2-Cyclohexen-1-ol	$C_6H_{10}O$	--	0.79	--
2-Cyclopenten-1-one, 2-hydroxy-3-methyl-	$C_6H_8O_2$	--	0.98	--
Oxazolidine, 2,2-diethyl-3-methyl-	$C_8H_{17}NO$	--	7.01	--
Thiophene, 2-butyltetrahydro-	$C_8H_{16}S$	--	1.01	--
Benzene, 1-ethoxy-4-ethyl-	$C_{10}H_{14}O$	--	0.36	--
Naphthalene, 2-methyl-	$C_{11}H_{10}$	--	0.33	--
Biphenyl	$C_{12}H_{10}$	--	0.35	--
Biphenyl	$C_{12}H_{10}$	--	0.42	--
Total				

Ketones formed from the decomposition of hemicellulose. The content of ketones increased with temperature rising from 10.42 to 14.39%. CO_2 enhanced the deoxygenation reaction to produce the least carboxylic and carbonyl carbons. At higher temperature, the content of CO_2 was reduced, and the higher content CO and H_2 in the pyrolysis atmosphere had a positive effect on the ketone formation.

Table 4. Chemical Compounds of Heavy Bio-oil

No.	Compound	Formula	Area%
1	Phenol, 4-methyl-	C_7H_8O	0.36
2	N-Butyl-tert-butylamine	$C_8H_{19}N$	1.32
3	Benzo[b]thiophene, 6-methyl-	C_9H_8S	0.40
4	Phenol, 4-ethyl-2-methoxy-	$C_9H_{12}O_2$	0.68
5	2-Propenoic acid, 3-(2-hydroxyphenyl)-, (E)-	$C_9H_8O_3$	1.45
6	2-Methoxy-4-vinylphenol	$C_9H_{10}O_2$	3.37
7	3-Allyl-6-methoxyphenol	$C_{10}H_{12}O_2$	1.39
8	Phenol, 2-methoxy-6-(1-propenyl)-	$C_{10}H_{12}O_2$	0.80
9	Phenol, 2-methoxy-4-propyl-	$C_{10}H_{14}O_2$	0.41
10	Phenol, 2-methoxy-4-(1-propenyl)-	$C_{10}H_{12}O_2$	4.50
11	Benzene, 1,2,3-trimethoxy-5-methyl-	$C_{10}H_{14}O_3$	2.12
12	Phenol, 4-(3-hydroxy-1-propenyl)-2-methoxy-	$C_{10}H_{12}O_3$	2.85
13	4-Hydroxy-2-methoxycinnamaldehyde	$C_{10}H_{10}O_3$	0.98
14	Benzenemethanol, ar,ar,à-trimethyl-	$C_{10}H_{14}O$	0.50
15	Benzaldehyde, 2-hydroxy-3-(2-propenyl)-	$C_{10}H_{10}O_2$	0.47
16	Phenol, 2-methoxy-4-methyl-6-[propenyl]-	$C_{11}H_{14}O_2$	1.37
17	Phenol, 2,6-dimethoxy-4-(2-propenyl)-	$C_{11}H_{14}O_3$	2.81
18	Phenol, 2,6-dimethoxy-4-(2-propenyl)-	$C_{11}H_{14}O_3$	3.60
19	2-[(Benzo[1,3]dioxole-4-carbonyl)-amino]-3-hydroxy-propionic acid	$C_{11}H_{11}NO_6$	0.62
20	Benzoic acid, 4-(acetyloxy)-3-methoxy-, methyl ester	$C_{11}H_{12}O_5$	0.56
21	Salsoline	$C_{11}H_{15}NO_2$	0.47
22	Phosphine, (pentamethylphenyl)-	$C_{11}H_{17}P$	0.41
23	1,2-Dimethoxy-4-n-propylbenzene	$C_{11}H_{16}O_2$	0.39
24	Phenylethylene, 2-nitro-2',3',4',5'-tetramethoxy-	$C_{12}H_{15}NO_6$	0.62
25	Cyclopentanecarboxylic acid, 3-methylene-5-prop-2-enoic acid, dimethyl ester	$C_{12}H_{16}O_4$	0.33
26	Trimethoxyamphetamine, 2,3,5-	$C_{12}H_{19}NO_3$	2.19
27	1-Propyl-3,6-diazahomoadamantan-9-ol	$C_{12}H_{22}N_2O$	1.75
28	Isoquinoline, 1-[3-methoxy-5-hydroxybenzyl]-1,2,3,4-tetrahydro-	$C_{18}H_{21}NO_3$	2.68
29	2H-1-Benzopyran-3,4-diol, 2-(3,4-dimethoxyphenyl)-3,4-dihydro-6-methyl-, (2à,3à,4à)-	$C_{18}H_{20}O_5$	7.48
30	à-D-Glucopyranoside, O-à-D-glucopyranosyl-(1.fwdarw.3)-á-D-fructofuranosyl	$C_{18}H_{32}O_{16}$	2.77
31	2H-1-Benzopyran-3,4-diol, 2-(3,4-dimethoxyphenyl)-3,4-dihydro-6-methyl-, (2à,3à,4à)-	$C_{18}H_{20}O_5$	7.7
32	3-Benzofuranmethanol, 2,3-dihydro-2-(4-hydroxy-3-methoxyphenyl)-5-(3-hydroxy-1-propenyl	$C_{20}H2_2O_6$	3.42
33	Benzoic acid, 2-hydroxy-3-[(2-hydroxy-4-methoxy-6-propylbenzoyl)oxy]-4-methoxy-6-propyl	$C_{23}H_{28}O_8$	4.35
34	4,13,20-Tri-O-methylphorbol 12-acetate	$C_{25}H_{36}O_7$	2.67
35	Benzene, 1,1'-tetradecylidenebis	$C_{26}H_{38}$	3.50
36	Benzene, 1,1',1'',1'''-(1,6-hexanediylidene)tetrakis-	$C_{30}H_{30}$	1.03

Furans are produced by the decomposition of cellulose and hemicellulose. The main components include furfural, 3-furaldehyde, 2-furanmethanol, and 2(5h)-furanone. The content of furans in bio-oil increased sharply, which may be closely related to the atmosphere of CO and CO_2. The specific mechanism resulting in this change remains unclear. Esters and nitrogen compounds changed slightly at different temperatures, representing the contents of less than 8% and 5.5%, respectively.

The relative content of sugars decreased with increasing temperature. Sucrose and levoglucosan (LG) were the main components of bio-oil. LG was evidenced as one typical product from the cracking of cellulose pyrolysis (Yang *et al*. 2007; Shen *et al*. 2015). Higher temperatures promoted the depolymerization of macromolecule saccharides, which were converted into small organic matters. The yield of saccharides was highest at 450 °C.

The heavy bio-oil mainly contained mostly macromolecule organic compounds, as shown in Table 4. Partial phenols were detected, which may be caused by adhesion or dissolvability. The heavy bio-oil has a bad fluidity and contained partial fine char particles. Therefore, the heavy bio-oil was difficult to analyze unless it was purified through further methods.

CONCLUSIONS

1. A novel fluidized bed reactor with recycled gases as carrier media was designed, and the capacity of it reached 5 kg/h. The test of stability of pyrolysis process was conducted, and primary results of birch wood pyrolysis were obtained. The process can be continuously run for a long time (about 10 h).
2. In the range of 450 °C to 500 °C, the yield of bio-oil first increased and then decreased. The yield of gas increased with increasing temperature. The main components of NCG were CO and CO_2, and the relative total content of these gases was up to 86 vol.% at 450 °C. Because the contents of CO, CH_4, and H_2 increased with temperature rising, the HHV of NCG reached up to 11.2 MJ/m³.
3. The NCG had a significant effect on the pyrolysis process and favored the decomposition of vapor at high temperature. However, the specific mechanism of reaction remains unclear. Further work needs to be done to improve the automatization of the pyrolysis process, to achieve auto-regulation of rotation of the fan according the initial pressure of the process.

ACKNOWLEDGEMENTS

The authors are grateful for support from the Project supported by Shandong Provincial Natural Science Foundation of China (ZR2017MEE004), National Natural Science Foundation of China (51536009 and 51276103), Distinguished Expert of Taishan Scholars (Shandong Province) and Higher Education Superior Discipline Team Training Program of Shandong Province, China National Natural Science Fund (51606113), and Key Research and Development Program of Shandong Province (No. 2017GGX40108).

REFERENCES CITED

ASTM E871-82(2019). "Standard test method for moisture analysis of particulate wood fuels," ASTM International, West Conshohocken, USA.

ASTM E872-82(2019). "Standard test method for volatile matter in the analysis of particulate wood fuels," ASTM International, West Conshohocken, USA.

ASTM E1755-01(2015). "Standard test method for ash in biomass," ASTM International, West Conshohocken, USA

ASTM D2015-00(2000), "Standard test method for gross calorific value of coal and coke by the adiabatic bomb calorimeter (withdrawn 2000)," ASTM International, West Conshohocken, USA

Abraham, R., George, J., Thomas, J., and Yusuff, K. K. M. (2013). "Physicochemical characterization and possible applications of the waste biomass ash from oleoresin industries of India," *Fuel* 109, 366-372. DOI: 10.1016/j.fuel.2013.02.067

Azargohar, R., Jacobson, K. L., and Powell, E. E. (2013). "Evaluation of properties of fast pyrolysis products obtained from Canadian waste biomass," *Journal of Analytical and Applied Pyrolysis* 104, 330-340. DOI: 10.1016/j.jaap.2013.06.016

Bridgwater, A. V. (2012). "Review of fast pyrolysis of biomass and product upgrading," *Biomass Bioenergy* 38, 68-94. DOI: 10.1016/j.biombioe.2011.01.048

Collard, F. X., and Blin, J. (2014). "A review on pyrolysis of biomass constituents: Mechanisms and composition of the products obtained from the conversion of cellulose, hemicelluloses and lignin," *Renewable and Sustainable Energy Reviews* 38, 594-608. DOI: 10.1016/j.rser.2014.06.013

Choudhury, N. D., Chutia, R. S., Bhaskar, T., and Kataki, R. (2014). "Pyrolysis of jute dust: effect of reaction parameters and analysis of products," *Journal of Material Cycles and Waste Management* 16(3), 16449-459. DOI: 10.1007/s10163-014-0268-4

Demiral, İ., and Kul, Ş. Ç. (2014). "Pyrolysis of apricot kernel shell in a fixed-bed reactor: Characterization of bio-oil and char," *Journal of Analytical and Applied Pyrolysis* 107, 17-24. DOI: 10.1016/j.jaap.2014.01.019

Fernandez-Akarregi, A. R., Makibar, J., and Lopez, G. (2013). "Design and operation of a conical spouted bed reactor pilot plant (25 kg/h) for biomass pyrolysis," *Fuel Processing Technology* 112, 48-56. DOI: 10.1016/j.fuproc.2013.02.022

Hagner, M., Hallman, S., Jauhiainen, L., Kemppainen, R., Rämö, S., Tiilikkala, K., and Setälä H. (2015). "Birch (*Betula* spp.) wood biochar is a potential soil amendment to reduce glyphosate leaching in agricultural soils," *Journal of Environmental Management* 164, 46-52. DOI: 10.1016/j.jenvman.2015.08.039

Heo, H. S., Park, H. J., Park, Y., Ryu, C. K., Suh, D. J., Suh, Y., Yim, J., and Kim, S. (2010). "Bio-oil production from fast pyrolysis of waste furniture sawdust in a fluidized bed," *Bioresource Technology* 101, S91-S96. DOI: 10.1016/j.biortech.2009.06.003

Hu, S., Jiang, L., and Wang, Y. (2015). "Effects of inherent alkali and alkaline earth metallic species on biomass pyrolysis at different temperatures," *Bioresource Technology* 195, 23-30. DOI: 10.1016/j.biortech.2015.05.042

Isahak, W. N. R. W., Hisham, M. W. M., Yarmo, M. A., and Hin, T. Y. (2012). "A review on bio-oil production from biomass by using pyrolysis method," *Renewable and Sustainable Energy Reviews* 16, 5910-5923. DOI: 10.1016/j.rser.2012.05.039

Jung, S. H., Kang, B. S., and Kim, J. S. (2008). "Production of bio-oil from rice straw and bamboo sawdust under various reaction conditions in a fast pyrolysis plant

equipped with a fluidized bed and a char separation system," *Journal of Analytical and Applied Pyrolysis* 82, 240-247. DOI: 10.1016/j.jaap.2008.04.001

Jung, S. H., Kim, S. J., and Kim, J. S. (2012). "Characteristics of products from fast pyrolysis of fractions of waste square timber and ordinary plywood using a fluidized bed reactor," *Bioresource Technology* 114, 670-676. DOI: 10.1016/j.biortech.2012.03.044

Kan, T., Strezov, V., and Evans, T. J. (2016). "Lignocellulosic biomass pyrolysis: A review of product properties and effects of pyrolysis parameters," *Renewable and Sustainable Energy Reviews* 57, 1126-1140. DOI: 10.1016/j.rser.2015.12.185

Khelfa, A., Bensakhria, A., Weber, J. V. (2013), "Investigations into the pyrolytic behaviour of birch wood and its main components: Primary degradation mechanisms, additivity and metallic salt effects," *Journal of Analytical and Applied Pyrolysis* 101, 111-121. DOI: 10.1016/j.jaap.2013.02.004

Li, D. B., Berruti, F., and Briens, C. (2014). "Autothermal fast pyrolysis of birch bark with partial oxidation in a fluidized bed reactor," *Fuel* 121, 27-38. DOI: 10.1016/j.fuel.2013.12.042

Li, N., Wang, X., Bai, X. Y., Li, Zh. H., and Zhang, Y. (2015). "Biomass fast pyrolysis for bio-oil production in a fluidized bed reactor under hot flue atmosphere," *Chinese Journal Biotechnology* 31, 1501-1511.

Li, Zh. H., Li, N., Yi, W. M., Fu, P., Li, Y. J., and Bai, X. Y. (2017). "Design and operation of a down-tube reactor demonstration plant for biomass pyrolysis," *Fuel Processing Technology* 161, 182-192. DOI: 10.1016/j.fuproc.2016.12.014

Liu, S. J., Yi, W. M., Bai, X. Y., Wang, L. H., Yin, Zh., and Wu, J. (2009). "Experimental study on biomass fast pyrolysis in fluidized bed and analysis of bio-oil," *Transactions of the CSAE* 25, 203-207.

Lu, Q., Yang, X. L., and Zhu, X. F. (2008). "Analysis on chemical and physical properties of bio-oil pyrolyzed from rice husk," *Journal of Analytical and Applied Pyrolysis* 82, 191-198. DOI: 10.1016/j.jaap.2008.03.003

Mante, O. D., Agblevor, F. A., Oyama, S. T., and McClung, R. (2012). "The influence of recycled non-condensable gases in the fractional catalytic pyrolysis of biomass," *Bioresource Technology* 111, 482-490. DOI: 10.1016/j.biortech.2012.02.015

Paenpong, Ch., and Pattiya, A. (2016). "Effect of pyrolysis and moving-bed granular filter temperatures on the yield and properties of bio-oil from fast pyrolysis of biomass," *Journal of Analytical and Applied Pyrolysis* 119, 40-51. DOI: 10.1016/j.jaap.2016.03.019

Pattiya, A., and Suttibak, S. (2012). "Production of bio-oil via fast pyrolysis of agricultural residues from cassava plantations in a fluidised-bed reactor with a hot vapour filtration unit," *Journal of Analytical and Applied Pyrolysis* 95, 227-235. DOI: 10.1016/j.jaap.2012.02.010

Pattiya, A. (2011). "Bio-oil production via fast pyrolysis of biomass residues from cassava plants in a fluidised-bed reactor," *Bioresource Technology*, 102, 1959-1967. DOI: 10.1016/j.biortech.2010.08.117

Phan, B. M. Q., Duong, L. T., Nguyen, V. D., Tran, T. B., Nguyen, M. H. H., Nguyen, L. H., Nguyen, D. A., and Luu, L. C. (2014). "Evaluation of the production potential of bio-oil from Vietnamese biomass resources by fast pyrolysis," *Biomass Bioenergy* 62, 74-81. DOI: 0.1016/j.biombioe.2014.01.012

Raja, S. A., Kennedy, Z. R., Pillai, B. C., and Lee, C. L. R. (2010). "Flash pyrolysis of jatropha oil cake in electrically heated fluidized bed reactor," *Energy* 35, 2819-2823.

DOI: 10.1016/j.energy.2010.03.011
Sellin, N., Krohl, D. R., Marangoni, C., and Souza, O. (2016). Oxidative fast pyrolysis of banana leaves in fluidized bed reactor, *Renewable Energy* 96, 56-64. DOI: 10.1016/j.renene.2016.04.032
Shen, D. K., Jin, W., and Hu, J. (2015). "An overview on fast pyrolysis of the main constituents in lignocellulosic biomass to valued-added chemicals: Structures, pathways and interactions," *Renewable and Sustainable Energy Reviews* 51, 761-774. DOI: 10.1016/j.rser.2015.06.054
Tripathi, M., Sahu, J. N., and Ganesan, P. (2016). "Effect of process parameters on production of biochar from biomass waste through pyrolysis: A review," *Renewable and Sustainable Energy Reviews* 55, 467-481. DOI: 10.1016/j.rser.2015.10.122
Vassilev, S. V., Baxter, D., Andersen, L. K., and Vassileva, C. G. (2010). "An overview of the chemical composition of biomass," *Fuel* 89, 913-933. DOI: 10.1016/j.fuel.2009.10.022
Wang, X. (2015). *Experimental Study on the Flow Characteristics of Particles in Fluidized Bed*, Master's Thesis, Shandong University of Technology, Zibo.
Yan, R., Yang, H. P., Chin, T., Liang, D. T., Chen, H. P., and Zheng, Ch. G. (2005). "Influence of temperature on the distribution of gaseous products from pyrolyzing palm oil wastes," *Combustion and Flame* 142, 24-32. DOI: 10.1016/j.combustflame.2005.02.005
Yang, H. P., Yan, R., and Chen, H. P. (2007). "Characteristics of hemicellulose, cellulose and lignin pyrolysis," *Fuel* 86, 1781-1788. DOI: 10.1016/j.fuel.2006.12.013
Yi, W. M., Liu, S. J., Bi, D. M., Bai, X. Y., and Li, Zh. H. (2011). "Influence of temperature and bed materials on biomass pyrolysis product distribution," *Acta Energiae. Solaris Sinica* 32, 25-30.
Zhao, Ch. X., Jiang, E. Ch., and Chen, A. H. (2016). "Volatile production from pyrolysis of cellulose, hemicellulose and lignin," *Journal of the Energy Institute* 90(6), 1-12. DOI: 10.1016/j.joei.2016.08.004
Zhang, D. L. (2012). *Design and Experiment on Down Flow Tube Reactor for Biomass Pyrolysis Liquefaction*, Master's Thesis, Shandong University of Technology, Zibo.
Zhang, H. Y., Xiao, R., Wang, D. H., He, G. Y., Shao, S., Zhang, J. B., and Zhong, Z. P. (2011). "Biomass fast pyrolysis in a fluidized bed reactor under N_2, CO_2, CO, CH_4 and H_2 atmospheres," *Bioresource Technology* 102, 4258-4264. DOI: 10.1016/j.biortech.2010.12.075
Zhang, L. H., Xu, Ch. B., and Champagne, P. (2010). "Overview of recent advances in thermo-chemical conversion of biomass," *Energy Conversion and Management* 51, 969-982. DOI: 10.1016/j.enconman.2009.11.038

Article submitted: May 25, 2019; Peer review completed: July 29, 2019; Revised version received and accepted: August 17, 2019: Published: August 22, 2019.
DOI: 10.15376/biores.14.4.8114-8134